The Astrophysical Journal Letters, 899:L32 (9pp), 2020 August 20 https://doi.org/10.3847/2041-8213/abaaa9

Effects of Solar Activity on Taylor Scale and Correlation Scale in Solar Wind Magnetic Fluctuations

G. Zhou[1,2], H.-Q. He[1,3,4], and W. Wan[1,3,4]
[1] Key Laboratory of Earth and Planetary Physics, Institute of Geology and Geophysics, Chinese Academy of Sciences, Beijing 100029, People's Republic of China
hqhe@mail.iggcas.ac.cn
[2] College of Earth and Planetary Sciences, University of Chinese Academy of Sciences, Beijing 100049, People's Republic of China
[3] Innovation Academy for Earth Science, Chinese Academy of Sciences, Beijing 100029, People's Republic of China
[4] Beijing National Observatory of Space Environment, Institute of Geology and Geophysics, Chinese Academy of Sciences, Beijing 100029, People's Republic of China
Received 2020 June 1; revised 2020 July 28; accepted 2020 July 29; published 2020 August 19

Abstract

The correlation scale and the Taylor scale are evaluated for interplanetary magnetic field fluctuations from two-point, single time correlation function using the Advanced Composition Explorer (ACE), Wind, and Cluster spacecraft data during the time period from 2001 to 2017, which covers over an entire solar cycle. The correlation scale and the Taylor scale are respectively compared with the sunspot number to investigate the effects of solar activity on the structure of the plasma turbulence. Our studies show that the Taylor scale increases with the increasing sunspot number, which indicates that the Taylor scale is positively correlated with the energy cascade rate, and the correlation coefficient between the sunspot number and the Taylor scale is 0.92. However, these results are not consistent with the traditional knowledge in hydrodynamic dissipation theories. One possible explanation is that in the solar wind, the fluid approximation fails at the spatial scales near the dissipation ranges. Therefore, the traditional hydrodynamic turbulence theory is incomplete for describing the physical nature of the solar wind turbulence, especially at the spatial scales near the kinetic dissipation scales.

Unified Astronomy Thesaurus concepts: Solar wind (1534); Interplanetary turbulence (830); Interplanetary medium (825); Solar magnetic fields (1503); Space plasmas (1544); Solar activity (1475); Solar cycle (1487)

1. Introduction

Solar wind turbulence has received considerable attention for several decades within the community (e.g., Kraichnan 1965; Belcher 1971; Matthaeus & Goldstein 1982a, 1982b; Tu & Marsch 1995), and recently there has been an upsurge in interest in this topic. Much of the interest is driven by the fact that the solar wind can provide a perfect natural laboratory for the study of plasma turbulence in space at low-frequency magnetohydrodynamic (MHD) scales, which is essential for the studies of solar wind generation, plasma heating, energetic particle acceleration, cosmic-ray propagation, and space weather (Coleman 1968; Jokipii 1968a, 1968b; Matthaeus et al. 1984; Barnes 1979). During the past decades, the solar wind fluctuation properties and equations of motion have been studied in great detail (Belcher 1971; Matthaeus & Goldstein 1982a; Tu et al. 1984, 1989; Marsch & Tu 1997; Tu & Marsch 1997). However, even until now, it is still impossible to make accurate quantitative predictions. Most of the earlier studies used the single-spacecraft time-lagged data to infer solar wind spatial properties based on the well-known "frozen-in flow" approximation (Taylor 1938). Provided that the solar wind flow speed $\boldsymbol{V}_{\rm sw}$ is much greater than the local Alfvén speed $\boldsymbol{V}_{\rm A}$, the solar wind fluctuations that pass a detector are convected in a short time compared to all relevant characteristic dynamical timescales, so the time lags Δt are equivalent to spatial separations $\Delta t\boldsymbol{V}_{\rm sw}$. This assumption is relatively reliable under some specific conditions (Paularena et al. 1998; Ridley 2000). However, the timescale over which the frozen-in flow assumption remains valid is not fully established (Matthaeus et al. 2005; Weygand et al. 2013), and the correct way to establish the spatial structure is to make use of the simultaneous two-point single time measurements.

To overcome the shortcomings of the frozen-in flow assumption, Matthaeus et al. (2005) obtained the two-point correlation function making use of simultaneous two-point measurements of the magnetic fields. By using this technique, both the correlation length scale and the Taylor scale can be determined, and the values of these two scales were given to be 186 Re (Earth radius, 1 Re = 6378 km) and 0.39 ± 0.11 Re, respectively. Weygand et al. (2007) used the same method and obtained the Taylor scale values from the data of magnetic field fluctuations in plasma sheet and solar wind based on the Richardson extrapolation method. They estimated the Taylor scale in the solar wind as 2400 ± 100 km, which agrees with the value given by Matthaeus et al. (2005). Based on the two-point correlation measurement technique, Weygand et al. (2009) also obtained the values of the correlation scale and the Taylor scale by analyzing the magnetic field data measured from the magnetospheric plasma sheet and the solar wind. Their results showed that in the solar wind, the correlation scale along the magnetic field is longer than that along the perpendicular direction, and the Taylor scale is independent of the magnetic field directions. These conclusions indicated that the turbulence is anisotropic. Later, Matthaeus et al. (2010) provided a method for estimating the two-time correlation function and the associated Eulerian decorrelation timescale in the turbulence. This method can compare the two-point correlation measurements with the single-point measurements at corresponding spatial separations, and can be used for studying the temporal decorrelation of magnetic field fluctuations in space. Recently,

by using the direct two-point measurements and the frozen-in flow assumption, Chasapis et al. (2017) examined the second-order and fourth-order structure functions of the magnetic turbulence at very small scales in the solar wind. Their analysis extended several familiar statistical results, including the spectral distribution of energy and the scale-dependent kurtosis, down to the spatial scale near 6 km, and also clarified the earlier results.

All these applications of the two-point correlation measurements validate the excellent performance of this technique for studying the structure of the solar wind turbulence. In the current Letter we determine the values of correlation and Taylor scales of the interplanetary magnetic field fluctuations based on two-point single time correlation functions throughout a solar cycle to study the effects of solar activity on the structure of the plasma turbulence in the solar wind.

This Letter is organized as follows. In Section 2, we give a brief description of some basic concepts of the fluid turbulence, which can also be used in the field of plasma turbulence. In Section 3, we provide a detailed description of the method and the procedure of the two-point measurements. In Section 4, we calculate the Taylor scale and the correlation scale in different time ranges, and discuss how the solar activity influences the structure of the plasma turbulence. Several significant conclusions will be provided in Section 5.

2. Fundamental Concepts in Fluid Turbulence

A turbulent flow should satisfy the Navier–Stokes equation, which is the momentum evolution of an element of fluid and can be written as

$$\frac{\partial \boldsymbol{u}}{\partial t} + \boldsymbol{u}\cdot\nabla\boldsymbol{u} = -\frac{1}{\rho}\nabla p + \nu\nabla^2\boldsymbol{u}. \tag{1}$$

Here $\boldsymbol{u}$ is the velocity, which is a fluctuating quantity in time t and space $\boldsymbol{x}$, ∇ is the gradient with respect to $\boldsymbol{x}$, ρ is the density, p is the pressure, and ν is the kinematic viscosity. Note that Equation (1) corresponds to the incompressible case. Furthermore, Equation (1) neglects forces (driving forces, gravity) except pressure. The strength of the nonlinear convective term $\boldsymbol{u}\cdot\nabla\boldsymbol{u}$ against the dissipative term $\nu\nabla^2\boldsymbol{u}$ in Equation (1) can be measured by the "Reynolds number" which is defined as $R = UL/\nu$, where U and L denote the characteristic flow velocity and the characteristic length scale (or correlation scale in this study), respectively. The turbulent flow is characterized by large Reynolds numbers, which requires that the viscous term should be insignificant in this case. However, the boundary conditions or initial conditions may make it impossible to neglect the viscous term everywhere in the flow field. This can be understood by allowing for the possibility that viscous effects may be associated with the small length scales. Under the conditions of large Reynolds numbers, to make the dissipative term be the same order of the convective term, the viscous term can survive only by choosing a new length scale l. Thus,

$$U^2/L = \nu U/l^2. \tag{2}$$

From Equation (2), we can derive that

$$\frac{l}{L} \sim \left(\frac{\nu}{UL}\right)^{1/2} = R^{-1/2}. \tag{3}$$

The length scale l is called viscous length, which represents the width of the boundary layer. Thus, at very small length scales, the viscosity can be effective in smoothing out velocity fluctuations.

Since small-scale motions tend to have small timescales, one can assume that these motions are statistically independent of the relatively slow large-scale turbulence. If this assumption makes sense, the small-scale motion should depend only on the rate at which it is supplied with energy by the large-scale motion and on the kinematic viscosity. In accordance with Kolmogorov's universal equilibrium theory of the small-scale structure (Kolmogorov 1941a, 1941b), the rate of energy supply should be equal to the rate of dissipation. According to the dimensional analysis, the amount of the kinetic energy per unit mass in the turbulent flow is proportional to U^2; the rate of transfer of energy is proportional to $U/L \sim 1/T$, where T denotes the characteristic transfer time; the kinematic viscosity ν is proportional to $U\cdot L$; and the dissipation rate per unit mass ε, which should be equal to the supply rate, is proportional to $U^2/T \sim U^3/L$. With these parameters, we can obtain length, time, and velocity scales as $\eta \equiv (\nu^3/\varepsilon)^{1/4}$, $\tau \equiv (\nu/\varepsilon)^{1/2}$, and $v \equiv (\nu\varepsilon)^{1/4}$, respectively. These scales are known as the Kolmogorov microscales of length, time, and velocity. The Reynolds number formed with ν and v is $R_\eta = \eta v/\nu = 1$. The value $R_\eta = 1$ indicates that the small-scale motion is quite viscous, and that the viscous dissipation adjusts itself to the energy supply by adjusting length scales. From the expression

$$\varepsilon \sim U^3/L, \tag{4}$$

we know that the viscous dissipation of energy could be estimated from the large-scale dynamics that does not involve viscosity. Thus, the dissipation can be seen as a passive process in the sense that it proceeds at a rate dominated by the inviscid inertial behavior of the large eddies. The above expression is one of the cornerstone assumptions of the classical hydrodynamic turbulence. However, we should keep in mind that the large eddies only lose a negligible fraction of their energy compared to direct viscous dissipation effects. Supposing that the timescale of the energy decay is L^2/ν, then the energy loss proceeds at a rate of $\nu U^2/L^2$, which is very small compared to U^3/L if the Reynolds number $R = UL/\nu = \frac{U^3/L}{\nu U^2/L^2}$ is very large. Kolmogorov (1941a, 1941b) suggested that the small-scale structure of turbulence is always approximately isotropic when the Reynolds number is large enough. This is the well-known local isotropy theory. In isotropic turbulence, the dissipation rate can be simply expressed as

$$\varepsilon \sim \nu\frac{U^2}{\lambda^2}, \tag{5}$$

where λ denotes the Taylor scale. Combining Equations (4), (5), and the form of the Kolmogorov microscale, we can obtain

$$\frac{\lambda}{L} \sim \left(\frac{\nu}{UL}\right)^{1/2} = R^{-1/2}, \frac{\eta}{L} \sim \left(\frac{\nu}{UL}\right)^{3/4} = R^{-3/4},$$
$$\frac{\lambda}{\eta} \sim \left(\frac{UL}{\nu}\right)^{1/4} = R^{1/4}. \tag{6}$$

Comparing Equation (3) with Equation (6), we can see that the Taylor scale is related to the viscous dissipation. Equation (6) also suggests that for hydrodynamic turbulence with large

Reynolds number, the Taylor scale is larger than the Kolmogorov microscale.

The length scales L, η, and λ mentioned above can characterize the properties of the flow with high Reynolds numbers. The correlation scale L, also known as "outer" scale or "energy containing" scale, is related to the inertial range of the turbulence. This parameter represents the size of the largest eddy in the turbulent flow (Batchelor 1953; Tennekes & Lumley 1972; Batchelor 2000). The large eddies perform most of the transport of momentum and contaminants, and the energy input also occurs mainly at large scales. This correlation scale can be measured by classical methods based on the Taylor's hypothesis and can be associated with the first bendover point in the power spectrum of the turbulent fluctuations. The Kolmogorov microscale η ("inner" scale or dissipation scale) represents the smallest length scale in the turbulent flow (Jokipii & Hollweg 1970; Tennekes & Lumley 1972) and it is at the end of the inertial range. In the view of traditional hydrodynamics, the viscosity can be effective in smoothing out fluctuations and dissipates small-scale energy into heat at very small length scales (note that in the low-collisionality plasmas, this situation is less clear). A standard method for identifying the Kolmogorov microscale is to associate it with the breakpoint at the high-wavenumber end of the inertial range above which the spectral index of the power spectral density becomes steeper. The Taylor scale λ is first proposed by Taylor (1935). It can be associated with the curvature of the two-point magnetic field correlation function evaluated at zero separation (Tennekes & Lumley 1972; Matthaeus et al. 2005; Weygand et al. 2010, 2011; Chuychai et al. 2014). In contrast to the correlation scale and the Kolmogorov microscale, the Taylor scale does not represent any group of eddy size, but it can characterize the dissipative effects. Moreover, the Taylor scale is of the same order of magnitude as the Kolmogorov microscale. Specifically, the latter is often smaller than the former for hydrodynamic turbulence with large Reynolds numbers.

An essential characteristic of turbulence is the transfer of energy across scales. The energy resides mainly at large scales, but it can be transferred across scales by nonlinear processes, and eventually it arrives at small scales. The dissipation mechanisms at the small scales would limit the transfer, dissipate the fluid motions, and release the heat (Batchelor 1953; Tennekes & Lumley 1972). This is the so-called "cascade" process. When the associated Reynolds number and magnetic Reynolds number are large compared to unity, this process can be expected in hydrodynamics and in fluid plasma models such as MHD. In previous studies, the cascade process is investigated through spectral analysis or structure function analysis (Matthaeus & Goldstein 1982a, 1982b; Goldstein et al. 1994, 1995; Tu & Marsch 1995; Zhou et al. 2004). Many analysis methods describe the inertial range of scale properties using the well-known power law of Kolmogorov theory for fluids (Kolmogorov 1941a, 1941b) and its variants for plasmas (Kraichnan 1965). In hydrodynamics, the inertial range (or the self-similar range) mentioned above is typically defined extending from the correlation scale (where the turbulence contains most of the energy) down to the Kolmogorov microscale. In this work, we use the correlation scale L and the Taylor scale λ, instead of the correlation scale L and the Kolmogorov microscale η, to describe the properties of the solar wind turbulence since the Taylor scale can be measured relatively easily (Tennekes & Lumley 1972; Weygand et al. 2005).

3. Methods and Procedures

If the turbulence is homogeneous in space, then the means, variances, and correlation values of the fluctuations are independent of the choice of origin of the coordinate system (Batchelor 1953; Tennekes & Lumley 1972; Barnes 1979; Batchelor 2000). For a magnetic field $\boldsymbol{B}(\boldsymbol{x}, t) = \boldsymbol{B}_0 + \boldsymbol{b}$, the mean is $\langle \boldsymbol{B} \rangle = \boldsymbol{B}_0$, the fluctuation is $\boldsymbol{b} = \boldsymbol{B} - \boldsymbol{B}_0$, and the variance is $\sigma^2 = \langle |\boldsymbol{b}|^2 \rangle$. The two-point correlation coefficient is

$$R(\boldsymbol{r}) = \frac{1}{\sigma^2} \langle \boldsymbol{b}(\boldsymbol{x}) \cdot \boldsymbol{b}(\boldsymbol{x} + \boldsymbol{r}) \rangle. \quad (7)$$

Here $\boldsymbol{r}$ is the separation of two points $\boldsymbol{x}$ and $\boldsymbol{x} + \boldsymbol{r}$. For homogeneity, R and $\boldsymbol{B}_0$ are independent of position $\boldsymbol{x}$, though they may be weakly dependent on position in reality. The $\langle ... \rangle$ denotes an ensemble average. In homogeneous medium, the ensemble average is equivalent to a suitably chosen time-averaging procedure. For large $|\boldsymbol{r}|$, the well-behaved turbulence becomes uncorrelated and $R \to 0$.

The direction-averaged correlation scale is defined as (Matthaeus & Goldstein 1982a; Matthaeus et al. 2005)

$$L = \int_0^\infty R(r) dr. \quad (8)$$

In addition, the Taylor scale can also be associated with the curvature of $R(r)$ at the origin (see Matthaeus et al. 2005 and Weygand et al. 2007 for more details). Strictly speaking the scale defined in Equation (8) is the integral scale that is not necessarily equal to the bendover scale of the spectrum. However, this will not affect the conclusions in this work. The discussions of different scales and their relations to each other can be found in Shalchi (2020). A model correlation function with the correct asymptotic behavior is $R(r) \sim e^{-r/L}$, which has often been used as an approximation tool for estimating L (Matthaeus & Goldstein 1982a). Note that $R(r) = 1$ for $r = 0$ and $R \to 0$ for $r \to \infty$.

From the equations mentioned above, it is clear that the two-point correlation coefficient $R(r)$ plays an important role in determining the correlation scale L and the Taylor scale λ. In the following, we shall focus on the procedures for obtaining the $R(r)$, L, and λ from multi-spacecraft data.

The magnetic field data used in this work were obtained by the instruments on spacecraft ACE, Wind, and Cluster during the time period from 2001 January to 2017 December. Most of the distances between the ACE and Wind spacecraft are in the range of 20–500Re, and the Cluster interspacecraft separations during this period range from about 100 km to over 10,000 km. Since the spacecraft ACE and Wind orbit the Lagrangian point L1, which is about 1.5 million km from the Earth and 148.5 million km from the Sun, the information of the solar wind can be directly obtained by the spacecraft. The Cluster mission, which consists of four identical spacecraft at different positions, can provide the three-dimensional measurements of large-scale and small-scale phenomena in the near-Earth environment (Escoubet et al. 1997). Note that the four Cluster spacecraft are not always in the solar wind. Occasionally, the Cluster spacecraft are in the Earth's magnetosphere. Therefore, the data provided by the Cluster mission should be filtered before we use them.

The first step for investigating the spatial scales in the solar wind turbulence is to identify the time intervals during which the spacecraft were immersed in the solar wind. Table 1 shows the typical values of several solar wind parameters near 1 au. As we can see, the values of the magnetic field magnitude and

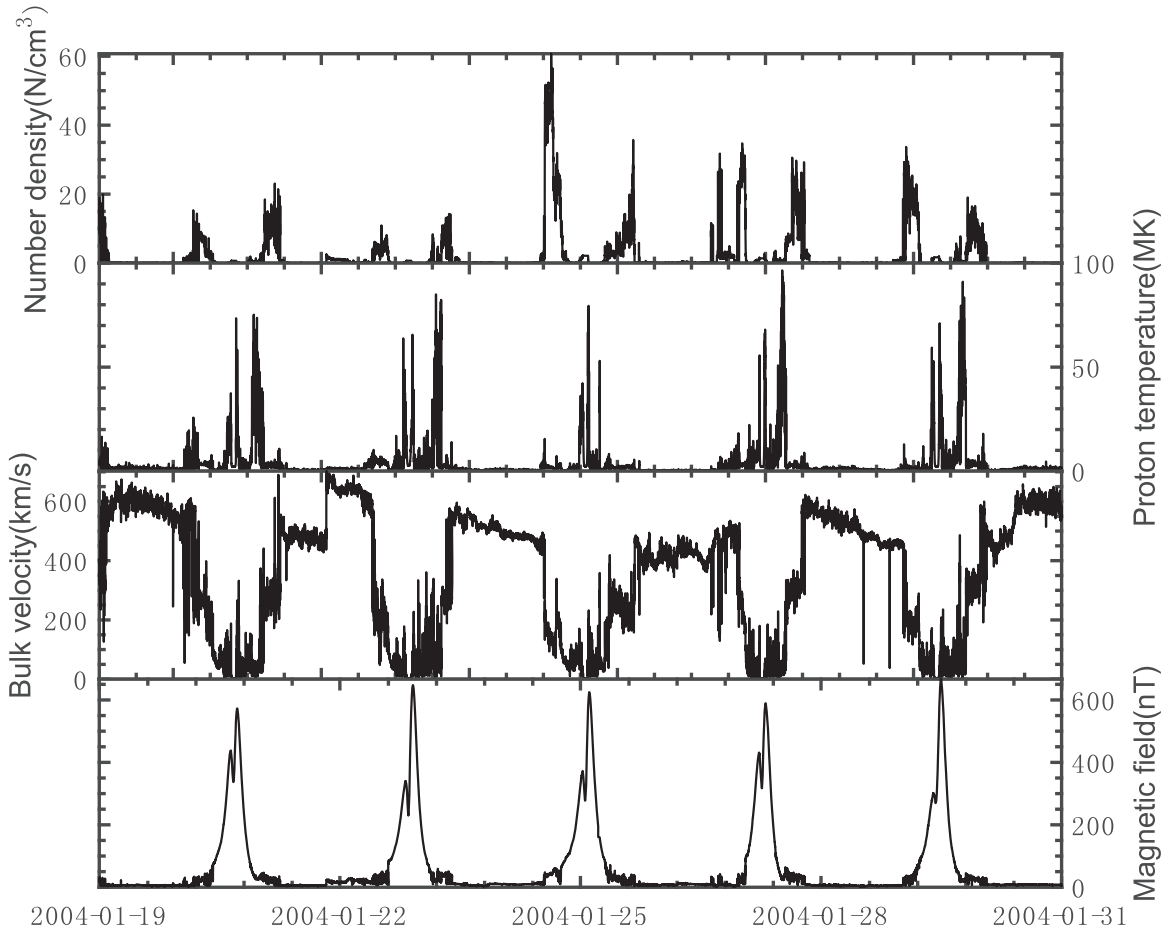

Figure 1. Time series of plasma data measured by FGM and CIS instruments on board Cluster 1 during the period 2004 January 19–31. The top, second, third, and bottom panels denote the particle number density, proton temperature, solar wind bulk velocity, and magnetic field magnitude, respectively.

Table 1
Typical Values of Several Solar Wind Parameters at 1 au

Solar Wind Parameters	Minimum Values	Maximum Values	Mean Values
Number density	0.04 cm^{-3}	8 cm^{-3}	5 cm^{-3}
Bulk velocity	200 km s^{-1}	900 km s^{-1}	400–500 km s^{-1}
Proton temperature	5×10^3 K	1×10^5 K	2×10^5 K
Magnetic field	0.25 nT	40 nT	6 nT

the plasma parameters drastically change when the spacecraft travel in and out of the Earth's magnetosphere. Generally, in the solar wind the plasma velocity is greater than 200 km s^{-1}, and the magnetic field magnitude is of the order of several *nT*. When the spacecraft fly into the Earth's magnetosphere, however, the plasma velocity decreases rapidly, and the magnetic field magnitude increases to several hundred *nT*. Furthermore, both the plasma number density and the proton temperature also show typically different values for different cases, namely, in the solar wind and in the magnetosphere.

To illustrate the difference in the measurements mentioned above, we take Figure 1 as an example. Figure 1 shows the time series of plasma data measured by the Fluxgate Magnetometer (FGM) and Cluster Ion Spectrometer experiment (CIS) instruments on board satellite Cluster 1 during the period 2004 January 19–31. In this time period, the satellite traveled in and out of the Earth's magnetosphere about 5 times. We can see the relatively regular variations of the plasma parameters in Figure 1. When the satellite crosses the magnetopause, the plasma number density rapidly increases due to the accumulation of particles there. The values of the proton temperature and the magnetic field magnitude also increase, while the plasma bulk velocity sharply decreases. When the satellite flies out of the magnetopause, however, these trends are reversed. Based on these behaviors, we can roughly distinguish the data intervals of the solar wind from those of the Earth's magnetosphere. In addition, an automated procedure can be adopted to identify the solar wind intervals. In our investigations, the solar wind shocks and other discrete solar wind structures are not removed from the data, since the time period studied is long enough to neglect the impacts of such solar wind structures.

The measurements from spacecraft ACE and Wind yield two-point correlation coefficients at larger separations, and those from the spacecraft Cluster provide the correlation coefficients at smaller separations. For each pair of the spacecraft, we linearly interpolated the data to 1 minute resolution to simultaneously obtain the field vectors at different spatial positions, since the sampling rate varied from spacecraft to spacecraft. In order to obtain meaningful two-point correlation coefficients at larger separations, longer continuous intervals are required for our analysis. Therefore, the ACE–Wind data are investigated with a cadence of 1 minute, and the individual correlation estimates are calculated by averaging over contiguous 24 hr periods of data. For Cluster data, the correlation analysis is carried out with 2 hr sampling.

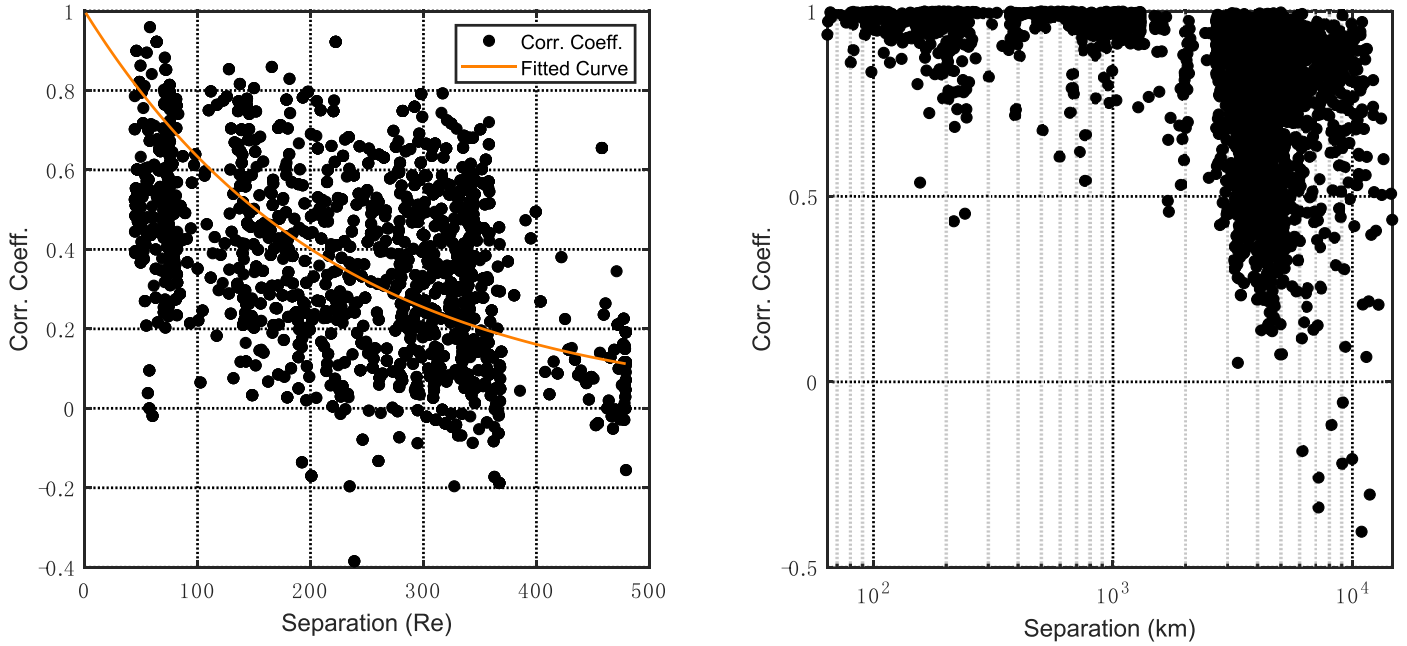

Figure 2. Estimates of solar wind normalized correlation coefficients $R(r)$ vs. spacecraft separations from ACE–Wind data intervals (left) and Cluster data intervals (right) during the years 2001–2003. The correlation coefficient for the magnetic field vectors decreases with the increasing spacecraft separation. Fitting to the ACE–Wind data (solid curve) in the left panel gives the correlation scale $L = 219$Re.

The data used in this study were measured during the time period 2001–2017 that covers over an entire solar cycle. The spacecraft can provide us thousands of time intervals for studying the effects of solar activity on the correlation scale and the Taylor scale. The entire data set is divided into a series of 3 yr time periods. In each 3 yr period, the data intervals are randomly selected. For each data interval, we calculate the time-averaged two-point correlation coefficients of the magnetic field vector. The correlation value is assigned to the time-averaged spacecraft distance in the corresponding interval. Using the normalized two-point correlation values calculated from a large number of solar wind measurements in different divided time periods, we can obtain the two-dimensional, normalized correlation coefficients as functions of the spatial separations and the time ranges. For example, Figure 2 shows the estimates of solar wind correlation coefficients $R(r)$ versus spacecraft separations from ACE–Wind data intervals (left) and Cluster data intervals (right) during the years 2001–2003. In the left panel of Figure 2, a mean correlation function with the form $R(r) \sim e^{-r/L}$ is obtained by fitting to the data of ACE–Wind correlation coefficients. Using the definition of the correlation scale L given by Matthaeus et al. (2005), i.e., $R(r) = e^{-1} = 0.368$, the (direction-averaged) correlation length scale L can be estimated to be 219 Re during the time period 2001–2003. We can use the so-called Richardson extrapolation technique (see Weygand et al. 2007 for details) to calculate the Taylor scale. Using the normalized correlation coefficients from Cluster data in the right panel of Figure 2, we can obtain that the Taylor scale is 4311.2 km during 2001–2003. Note that the data intervals are selected with a random procedure. Therefore, the correlation scale and the Taylor scale may slightly change their values when we repeat the calculations of them in the same divided time period. In this work, we use the averaged values of these repeated calculations for the correlation scale and the Taylor scale in each time period (2001–2003, 2002–2004, …, 2014–2016, 2015–2017).

We can employ the values in different time periods to investigate the variation trends of the correlation scale and the Taylor scale. In this work, the sunspot number is chosen to be the indicator of the solar activity. As we know, the number of sunspots varies with an 11 yr period, which is called the solar cycle (Parker 1979; Hathaway 2010). Generally, more sunspots indicate that more masses and energies would be released into interplanetary space through solar burst activities and events. By means of the data of the sunspot number, the correlation scale, and the Taylor scale, we can investigate the effects of the solar activity on the structure of solar wind turbulence.

4. Results and Discussion

Figure 3 displays the evolution of the sunspot number and the correlation scale during the time period 2001–2017. The left and right ordinates denote the sunspot number and the correlation scale, respectively. Obviously, the variation of the sunspots shows a regular and periodic trend. As we can see, the correlation scale also shows a weak periodic variation trend. When the sunspot number is large, the correlation scale becomes large; while when the sunspot number is small, the correlation scale becomes relatively small as well. For example, during the time periods 2001–2004 and 2011–2014, the sunspot number and the correlation scale are larger than those during the time periods 2005–2010 and 2014–2017. As shown in Figure 3, the maximum and the minimum of the correlation scale are 211.6 Re and 152.7 Re, respectively. The averaged value of the correlation scale for all time periods is 178.12 Re, which is similar to the value 186 Re given in Matthaeus et al. (2005). The correlation coefficient between the sunspot number and the correlation scale is 0.56, which suggests a moderate positive correlation between the solar activity and the correlation scale. That is to say, the correlation scale of the solar wind turbulence is modulated by the solar activity to some extent, but not significantly.

Figure 4 depicts the evolution features of the sunspot number and the Taylor scale during the time period 2001–2017. The

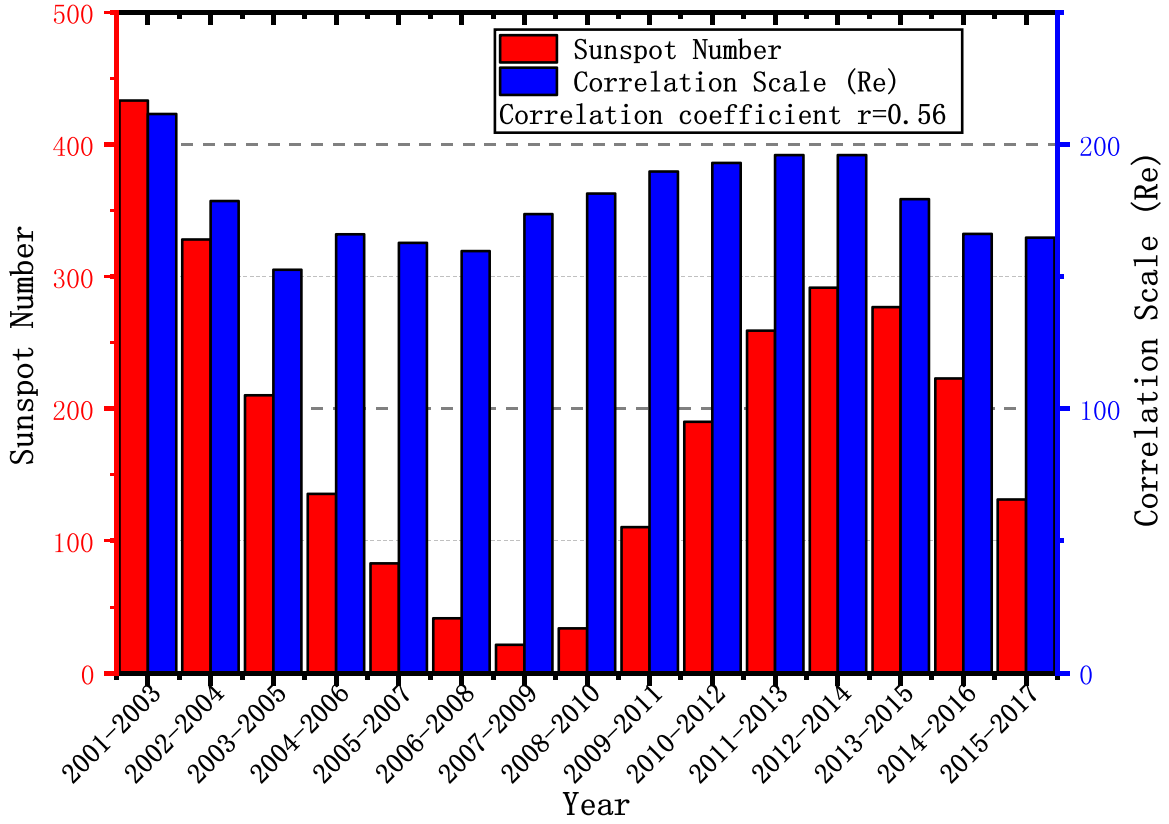

Figure 3. Evolution features of sunspot number (red) and correlation scale (blue) during time period 2001–2017. The left and right ordinates denote the sunspot number and the correlation scale (Re), respectively. The correlation coefficient between the sunspot number and the correlation scale is 0.56.

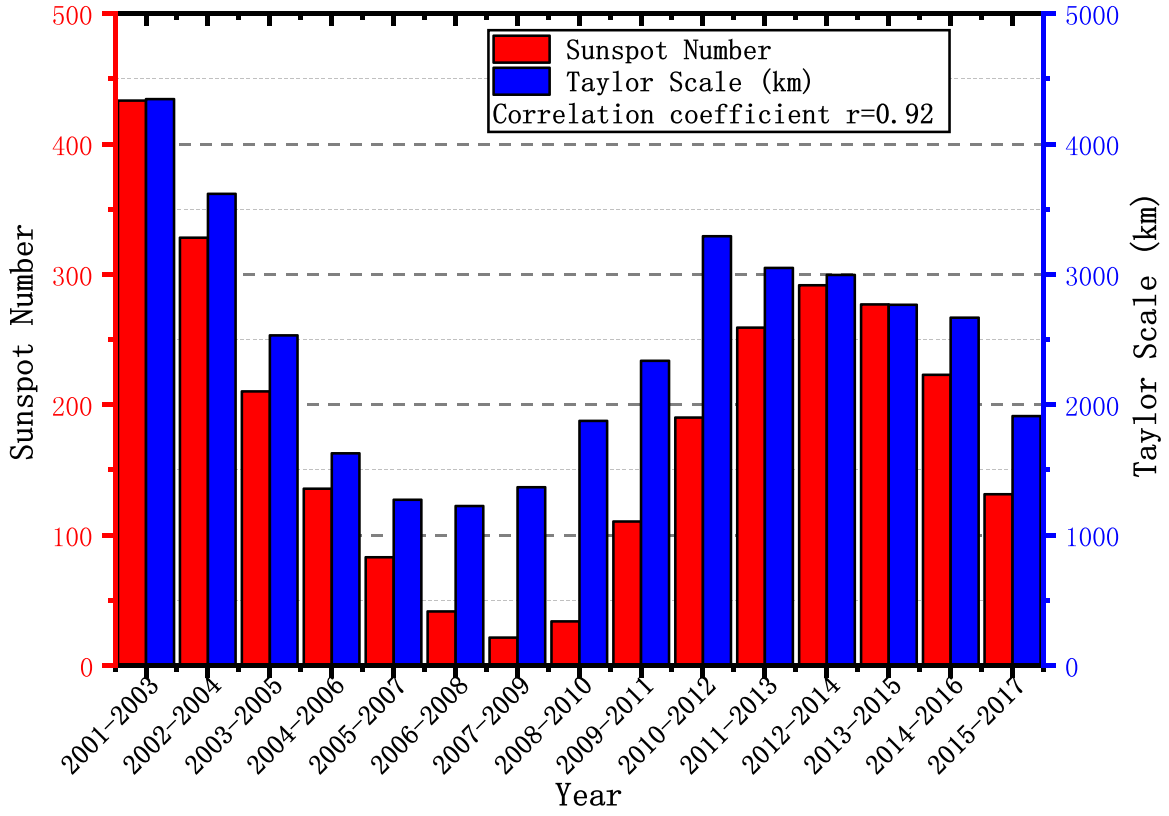

Figure 4. Evolution features of sunspot number (red) and Taylor scale (blue) during time period 2001–2017. The left and right ordinates denote the sunspot number and the Taylor scale (km), respectively. The correlation coefficient between the sunspot number and the Taylor scale is 0.92.

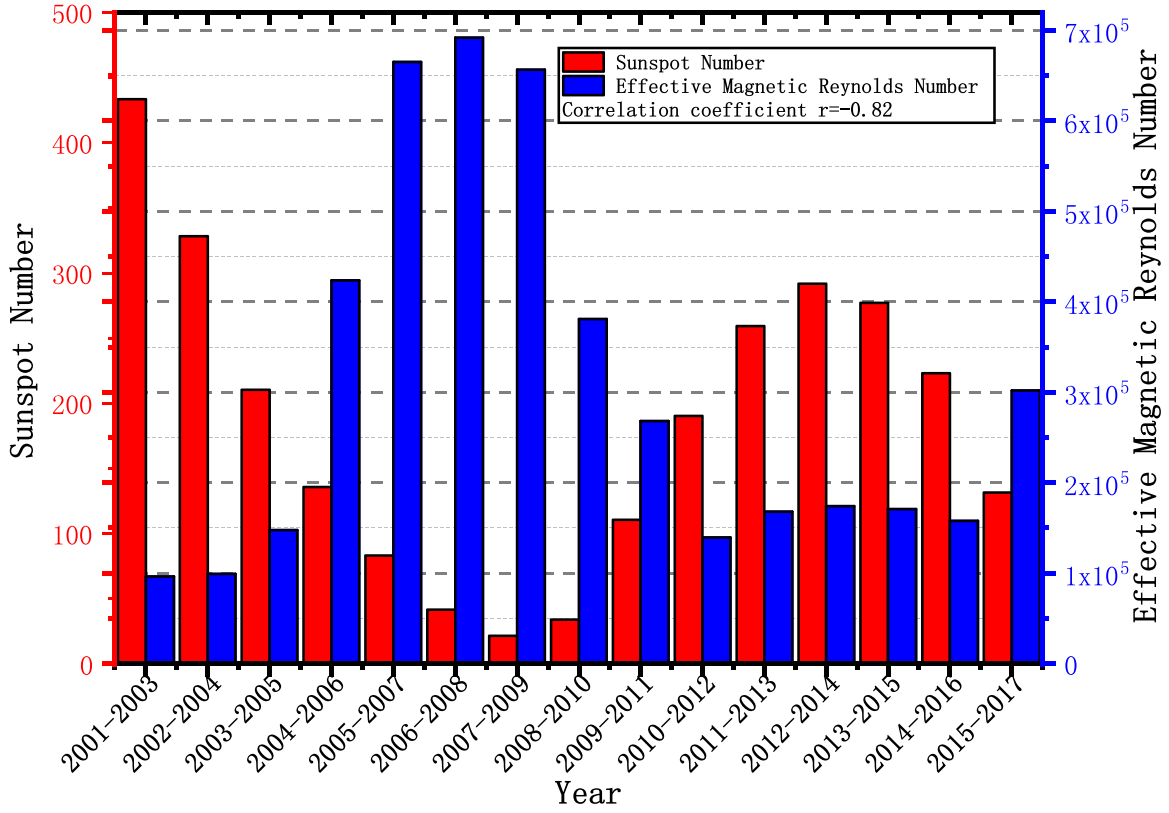

Figure 5. Evolution features of sunspot number (red) and effective magnetic Reynolds number (blue) during time period 2001–2017. The left and right ordinates denote the sunspot number and the effective magnetic Reynolds number, respectively. The correlation coefficient between the sunspot number and the effective magnetic Reynolds number is −0.82.

left and right ordinates denote the sunspot number and the Taylor scale, respectively. As one can see, relative to the correlation scale, the Taylor scale is more significantly related to the sunspot number and the solar activity. The Taylor scale increases or decreases with the increasing or decreasing sunspot number, respectively. As shown in Figure 4, the maximum and the minimum of the Taylor scale are 4345.5 km and 1224.5 km, respectively. The averaged value of the Taylor scale for all time periods is 2459.3 km (0.39 Re), which agrees well with the value 0.39 ± 0.11 Re given in Matthaeus et al. (2005) and the value 2400 ± 100 km presented in Weygand et al. (2007). The correlation coefficient between the sunspot number and the Taylor scale is 0.92, which indicates a strong positive correlation between the solar activity and the Taylor scale. The high value of the correlation coefficient means that the Taylor scale is significantly modulated by the solar activity.

Based on Equation (6), we can obtain the form of the effective magnetic Reynolds number $R_m^{\rm eff}$ as

$$R_m^{\rm eff} = \left(\frac{L}{\lambda}\right)^2. \tag{9}$$

Figure 5 presents the evolution features of the sunspot number and the effective magnetic Reynolds number calculated with Equation (9) during the time period 2001–2017. The left and right ordinates denote the sunspot number and the effective magnetic Reynolds number, respectively. As mentioned above, relative to the correlation scale, the Taylor scale shows a stronger positive correlation with the sunspot number. The effective magnetic Reynolds number shows a negative correlation with the sunspot number. The correlation coefficient between the sunspot number and the effective magnetic Reynolds number is −0.82, which indicates that the turbulence is relatively weak during the time period of strong solar activity. This result is somewhat counterintuitive.

Generally, the energy output from the Sun varies with the solar activity. The solar activities include solar flares, coronal mass ejections, extreme ultraviolet emissions, and X-ray emissions (Hathaway 2010). Based on the magnetic field data from the spacecraft ACE and Wind, we have found that both the magnitude and the standard deviation of the magnetic fields increase during the rise phase of the solar cycle, and decrease during the declining phase of the solar cycle. Therefore, the magnetic energy $\boldsymbol{B}^2$ increases with the increasing solar activity, and decreases with the decreasing solar activity. Taking into account Equation (4) and replacing the energy with the magnetic energy, we can know that if the correlation scale L does not change significantly, the energy dissipation rate ε will increase with the increasing magnetic energy $\boldsymbol{B}^2$ during the rise phase of the solar cycle. Combining this result with Equation (5), we can further derive that in the traditional theory of hydrodynamic turbulence, the Taylor scale λ will decrease with the increasing ε during the rise phase of the solar cycle, and the λ will increase with the decreasing ε during the declining phase of the solar cycle. Therefore, according to the traditional theory of hydrodynamic turbulence, there should be negative correlation between the solar activity and the Taylor scale. However, our results show that there is strong positive correlation between them.

This counterintuitive finding is somewhat identical with the results presented by Smith et al. (2006) and Matthaeus et al. (2008). In the previous studies, the authors employed the data

sets involving intervals from the magnetic cloud and noncloud situations in the solar wind to investigate the spectral properties in the dissipation range. They showed that the spectral form in the dissipation range is not consistent with the predictions of the hydrodynamic turbulence and its MHD counterparts. For instance, the Taylor scale is usually larger than the Kolmogorov microscale for the hydrodynamic turbulence with large Reynolds number. However, Matthaeus et al. (2008) suggested that under several conditions, the Taylor scale is smaller than the Kolmogorov microscale even if the magnetic Reynolds number is large enough. Therefore, the plasma dissipation function is not of the familiar viscous-resistive Laplacian form. They suggested that the steeper gradient of the dissipation range spectrum is associated with the stronger energy cascade rate. For weaker cascade rate, the gradient of the dissipation range spectrum is gentler. Here, the steep dissipation range spectrum indicates that the Taylor scale is large. On the contrary, the gentle dissipation range spectrum means that the Taylor scale is small. This result is similar to our finding that there exists positive correlation between the Taylor scale and the energy dissipation rate. This finding highlights the non-hydrodynamic properties of the dissipation process in the solar wind. One possible explanation is that in the solar wind, the assumption of the fluid approximation fails at the spatial scales near the dissipation range. Therefore, the traditional hydrodynamic turbulence theory is incomplete for describing the physical nature of the solar wind turbulence, especially at the spatial scales near the kinetic dissipation scales where the particle effects are not negligible. In the solar wind, the dissipation process of the turbulence always results from the breakdown of the fluid approximation and the domination of the kinetic particle effects such as cyclotron and Landau damping (Smith et al. 2006). Therefore, the dissipation process in the solar wind represents the coupling of the turbulent fluid cascade and the kinetic dissipation.

As the cornerstone assumption of the classical hydrodynamic turbulence, the viscous dissipation rate of energy can be estimated by the supply rate of energy at large scales. This assumption is described by Equation (4), and can be modified as

$$\varepsilon + \xi = U^3/L. \tag{10}$$

Here ε is the energy dissipation rate at small scales, U^3/L denotes the energy cascade rate, and ξ denotes the energy loss occurring when the energy transfers from large scales to small scales, especially near the spatial scales at which the solar wind fluid approximation fails. Equation (10) indicates that the sum of the energy dissipation rate and the total energy-loss rate equals the energy transfer rate. As shown above, the Taylor scale is strongly positively correlated with the energy cascade rate. Combining this result with Equation (5), we can infer that the Taylor scale λ will increase with the increasing magnetic energy U^2, which indicates that the energy dissipation rate ε is relatively stable in the solar wind turbulence. Therefore, the total energy loss ξ will increase with the increasing energy cascade rate U^3/L. Similarly, the total energy loss ξ will decrease with the decreasing energy cascade rate U^3/L. This finding sheds new light on the relationship between the energy cascade and the dissipation in the low-collisionality plasma turbulence.

5. Conclusions

In this work, based on the simultaneous measurements (Wind, ACE, and Cluster) of the interplanetary magnetic fields during the time period 2001 January–2017 December, we use the two-point, single time correlation function to determine the fundamental parameters of the solar wind turbulence, such as the correlation scale and the Taylor scale. The data set used in this study covers an entire solar cycle. It is possible to employ this data set accumulated over a long time period to study the effects of solar activity on the correlation scale and the Taylor scale. We show that the correlation coefficient between the sunspot number and the correlation scale is 0.56, and the correlation coefficient between the sunspot number and the Taylor scale is 0.92. Obviously, the relationship between the Taylor scale and the sunspot number is more significant than the relationship between the correlation scale and the sunspot number. Therefore, the effective magnetic Reynolds number is primarily affected by the Taylor scale. The correlation coefficient between the sunspot number and the effective magnetic Reynolds number is -0.82, which indicates that the solar wind turbulence is relatively weak when the solar activity is strong. This result is somewhat counterintuitive.

In traditional theory of hydrodynamic turbulence, the dissipation range or the inertial range can be described by a universal function. The dissipation scale is determined by the energy cascade rate through the inertial range. Specifically, the stronger cascades generate the smaller dissipation scales. However, our results suggest that the form of the dissipation process in solar wind turbulence is not consistent with the predictions of the hydrodynamic turbulence and its immediate MHD counterparts. Using the solar wind data measured at 1 au, we have shown that the variation of the Taylor scale depends on the energy cascade rate in a manner different from the traditional hydrodynamic case. The Taylor scale increases with the increasing sunspot number, and decreases with the decreasing sunspot number. This indicates that the Taylor scale is positively correlated with the energy cascade rate.

One possible explanation is that in the solar wind, the fluid approximation fails at the spatial scales near the dissipation range. Therefore, the traditional theory of hydrodynamic turbulence is incomplete for describing the physical nature of solar wind turbulence, especially at the spatial scales near the kinetic dissipation scale where the particle effects are not negligible. The dissipation process in the MHD turbulence results from the breakdown of the fluid approximation and the domination of the kinetic particle effects such as cyclotron and Landau damping. Therefore, the dissipation process in the solar wind represents the coupling of the turbulent fluid cascade and the kinetic dissipation. We suggest that the energy dissipation rate ε is relatively stable in solar wind turbulence. The energy cascade rate U^3/L is positively correlated with the total energy loss ξ.

The results presented in this work suggest that solar wind turbulence is influenced by the solar activity accompanying the solar cycle. In addition, our investigations highlight the non-hydrodynamic properties of the dissipation process in the solar wind, which provides new perspectives on the relationship between the energy cascade and the dissipation in the low-collisionality plasma turbulence. The anisotropy of the solar wind turbulence is another important subject in the field. In the future work, we will investigate the effects of the solar

activities and the solar cycle on the anisotropy of the solar wind turbulence.

This work was supported in part by the B-type Strategic Priority Program of the Chinese Academy of Sciences under grant XDB41000000, the National Natural Science Foundation of China under grants 41874207, 41621063, 41474154, and 41204130, and the Chinese Academy of Sciences under grant KZZD-EW-01-2. H.-Q.H. gratefully acknowledges the partial support of the Youth Innovation Promotion Association of the Chinese Academy of Sciences (No. 2017091). We benefited from the data of ACE, Wind, and Cluster provided by NASA/Space Physics Data Facility (SPDF)/CDAWeb. The sunspot data were provided by the World Data Center SILSO, Royal Observatory of Belgium, Brussels.

References

Barnes, A. 1979, in Solar System Plasma Physics, ed. E. N. Parker, C. F. Kennel, & L. J. Lanzerotti (Amsterdam: North-Holland), 249
Batchelor, G. K. 1953, The Theory of Homogeneous Turbulence (Cambridge: Cambridge Univ. Press)
Batchelor, G. K. 2000, An Introduction to Fluid Dynamics (Cambridge: Cambridge Univ. Press)
Belcher, J. W. 1971, ApJ, 168, 509
Chasapis, A., Matthaeus, W. H., Parashar, T. N., et al. 2017, ApJL, 844, L9
Chuychai, P., Weygand, J. M., Matthaeus, W. H., et al. 2014, JGRA, 119, 4256
Coleman, P. J., Jr. 1968, ApJ, 153, 371
Escoubet, C. P., Schmidt, R., & Goldstein, M. L. 1997, SSRv, 79, 11
Goldstein, M. L., Roberts, D. A., & Fitch, C. A. 1994, JGR, 99, 11519
Goldstein, M. L., Roberts, D. A., & Matthaeus, W. H. 1995, ARA&A, 33, 283
Hathaway, D. H. 2010, LRSP, 7, 1
Jokipii, J. R. 1968a, ApJ, 152, 799
Jokipii, J. R. 1968b, ApJ, 152, 997
Jokipii, J. R., & Hollweg, J. V. 1970, ApJ, 160, 745
Kolmogorov, A. N. 1941a, DoSSR, 30, 301
Kolmogorov, A. N. 1941b, DoSSR, 32, 16
Kraichnan, R. H. 1965, PhFl, 8, 1385
Marsch, E., & Tu, C.-Y. 1997, SoPh, 176, 87
Matthaeus, W. H., Ambrosiano, J. J., & Goldstein, M. L. 1984, PhRvL, 53, 1449
Matthaeus, W. H., Dasso, S., Weygand, J. M., et al. 2005, PhRvL, 95, 231101
Matthaeus, W. H., Dasso, S., Weygand, J. M., Kivelson, M. G., & Osman, K. T. 2010, ApJL, 721, L10
Matthaeus, W. H., & Goldstein, M. L. 1982a, JGR, 87, 6011
Matthaeus, W. H., & Goldstein, M. L. 1982b, JGR, 87, 10347
Matthaeus, W. H., Weygand, J. M., Chuychai, P., et al. 2008, ApJL, 678, L141
Parker, E. N. 1979, Cosmical Magnetic Fields: Their Origin and Their Activity (Oxford: Oxford Univ. Press)
Paularena, K. I., Zastenker, G. N., Lazarus, A. J., & Dalin, P. A. 1998, JGR, 103, 14601
Ridley, A. J. 2000, JASTP, 62, 757
Shalchi, A. 2020, SSRv, 216, 23
Smith, C. W., Hamilton, K., Vasquez, B. J., & Leamon, R. J. 2006, ApJL, 645, L85
Taylor, G. I. 1935, RSPSA, 151, 421
Taylor, G. I. 1938, RSPSA, 164, 476
Tennekes, H., & Lumley, J. L. 1972, First Course in Turbulence (Cambridge, MA: MIT Press)
Tu, C.-Y., & Marsch, E. 1995, SSRv, 73, 1
Tu, C.-Y., & Marsch, E. 1997, SoPh, 171, 363
Tu, C.-Y., Marsch, E., & Thieme, K. M. 1989, JGR, 94, 11739
Tu, C.-Y., Pu, Z.-Y., & Wei, F.-S. 1984, JGR, 89, 9695
Weygand, J. M., Kivelson, M. G., Khurana, K. K., et al. 2005, JGRA, 110, A01205
Weygand, J. M., Kivelson, M. G., Matthaeus, W. H., Dasso, S., & Kistler, L. M. 2007, AGU Fall Meeting (Washington, DC: AGU), SM23A-1197
Weygand, J. M., Matthaeus, W. H., Dasso, S., et al. 2009, JGRA, 114, A07213
Weygand, J. M., Matthaeus, W. H., Dasso, S., & Kivelson, M. G. 2011, JGRA, 116, A08102
Weygand, J. M., Matthaeus, W. H., El-Alaoui, M., Dasso, S., & Kivelson, M. G. 2010, JGRA, 115, A12250
Weygand, J. M., Matthaeus, W. H., Kivelson, M. G., & Dasso, S. 2013, JGRA, 118, 3995
Zhou, Y., Matthaeus, W. H., & Dmitruk, P. 2004, RvMP, 76, 1015